Direct Imaging of Spatially Varying Potential and Charge across Internal Interfaces in Solids

V. Ravikumar, R. P. Rodrigues, and Vinayak P. Dravid
Department of Materials Science and Engineering, Northwestern University, Evanston, Illinois 60208
(Received 10 April 1995)

Transmission electron holography is utilized to study the electrostatic potential and associated space charge across grain boundaries in $SrTiO_3$. While pristine boundaries show only the effect of a reduction in density of atoms, doped boundaries indicate the presence of potential barriers and associated space charge due to accumulation of charged point defects. This Letter demonstrates the viability of electron holography as a bulk sensitive tool to directly image and quantify the magnitude, sign, and spatial extent of electrical potential and charge across internal interfaces in solids.

PACS numbers: 61.72.Ff, 61.16.Bg, 61.72.Mm, 73.30.+y

Frenkel [1] in 1946 predicted a dipole region at ionic crystal surfaces (later extended to line and planar defects [2]) due to the presence of a surface charge and compensating space charge resulting from the differences in free energy of formation of point defects. Internal interfaces where at least one phase is nonconducting decorate themselves with charged defects and accumulate compensating (opposite) charge leading to a space-charge potential across the interface. This phenomenon plays a key role in technologically important systems, especially those containing electrically active interfaces, e.g., *p-n* junctions in semiconductors [3] and grain boundaries (GBs) in electroceramics [4]. Space charge at electroceramic interfaces has been indirectly deduced from measuring bulk properties via *I-V*, *C-V* curves and impedance spectroscopy [4]. While attempts have been made to determine the potential barrier height of *p-n* junctions [5] and leakage fields [6] in semiconductors, direct imaging of electrostatic potential profile and determination of the sign, magnitude, and distribution of the associated interface and space charge (and therefore defect density) in electroceramics have remained elusive for many decades.

Space charge and dopant segregation to the interface are interrelated, as they influence each other. Electroceramics such as varistors [4,7] are usually doped with aliovalent solutes to modify the space charge and thereby the electrical activity at the GB. A large number of researchers have pursued the identification of this relationship and analyze electrostatic potential and charge profile at such interfaces [4,7,8]. Deriving the local defect population from cation concentration profiles obtained by x-ray or electron energy loss spectroscopy (EELS) microanalysis across GBs [4,7] is suspect since the connection between chemical profiles and defect chemistry is usually not obvious. Also the local defect chemistry at the GB core is not well understood, and the results suffer from preconceived notions of dominating defects. Scanning tunneling spectroscopy (STS) of GBs [8] is a more direct technique; however, it probes only the surface and is thus not bulk sensitive. Also, tip-induced space charge in STS poses considerable problems in interpretation of the spectroscopy data. We have utilized transmission electron holography to directly image and quantify the barrier height and the local charge density distribution across grain boundaries in $SrTiO_3$, a functional electroceramic material. The results forecast a realistic opportunity to probe the statics and dynamics of electrostatic field and charge distribution across interfaces in technologically useful materials.

Electron holography, a coherent interferometry technique based on interference of a reference wave with a scattered wave, is directly sensitive to the potentials in solids. Using a Möllenstedt-type biprism [9] (placed in the plane of the selected area aperture and rotatable through 360° in this plane perpendicular to the optic axis) in a cold field emission transmission electron microscope operated at 200 keV, a reference wave and a scattered object wave are allowed to interfere, forming an interference fringe pattern that contains information on the phase and amplitude of the scattered wave. The phase of the electron wave at the GB region can be altered by [5,6,10,11]: (i) variation in local mean inner potential (related to the change in density of atoms at the GB), (ii) differential diffraction conditions across the interface, (iii) change in the local specimen thickness, and (iv) presence of local electrostatic (electrical charge) and magnetic field (see Fig. 1). In a

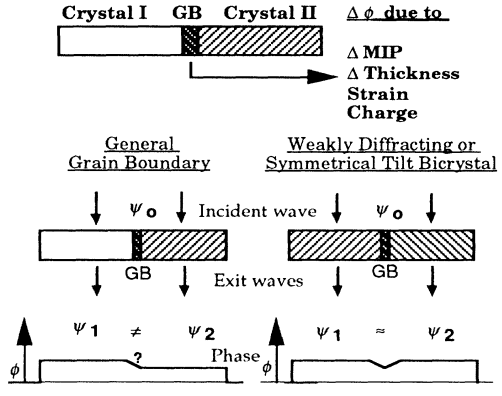

FIG. 1. Various contributions to the change in phase at GB. By using a symmetric tilt bicrystal or by making sure that both crystals are very weakly diffracting, phase changes due to differential diffraction of either grain can be minimized.

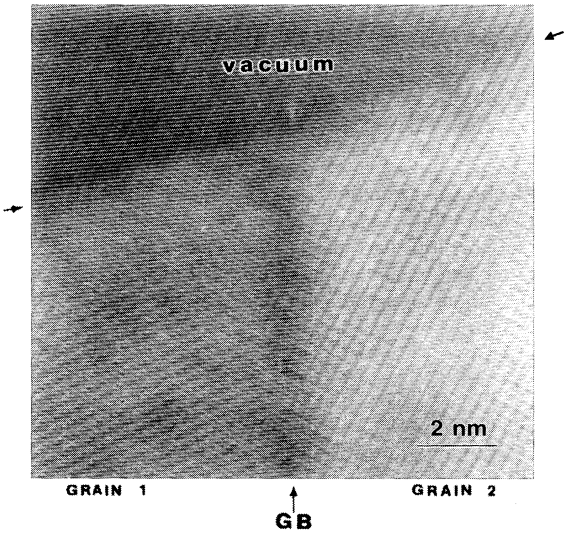

FIG. 2. An electron hologram of an undoped $\Sigma = 5$ (310) symmetrical tilt GB in $SrTiO_3$. Hologram interference fringe spacing $\approx$0.09 nm.

general case of crystalline interfaces, interpreting the local interface effects from GB core-region holograms is difficult because of nonidentical and strong diffraction conditions across the interface. However, under weak diffraction conditions, or certainly in the case of tilt bicrystals (where the exit wave functions are expected to be identical for either crystal), the differential phase change across the GB due to diffraction is minimal, and the changes in the phase of electron at and in the vicinity of the GB can be related to the other effects. The details regarding the theory and data analysis for electron holography have been described elsewhere [10,12].

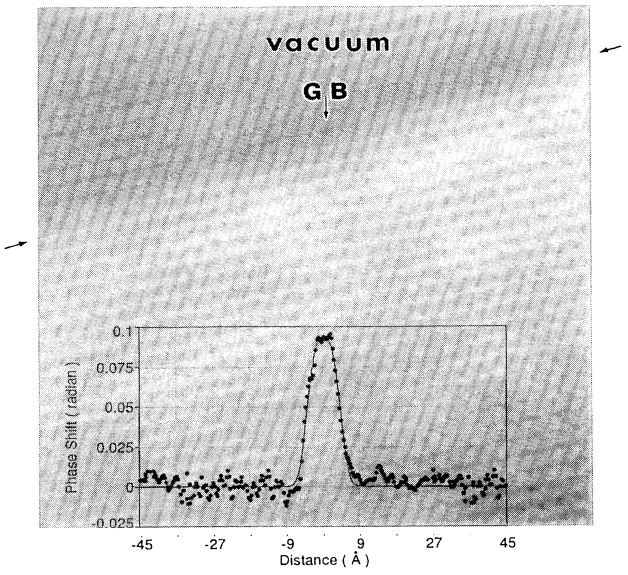

FIG. 3. Phase reconstruction of the hologram in Fig. 2. The averaged line scan of the phase across the GB is shown as an inset.

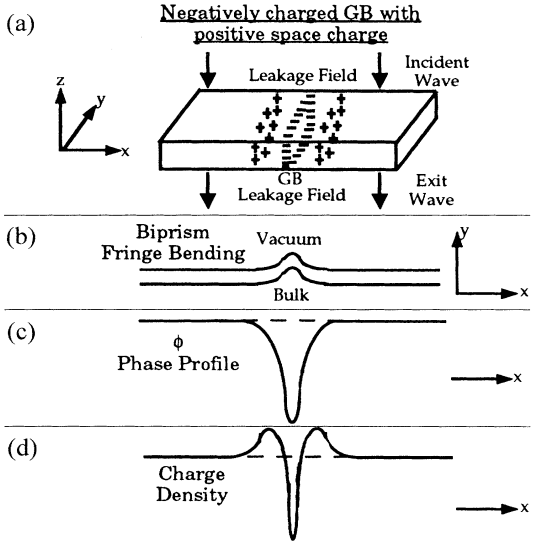

FIG. 4. Schematic for the case of a negatively charged GB with positive space charge (a). As shown, interference fringes bend towards vacuum (b) due to a decrease in phase (c) of electrons at the GB core. The charge density profile (d) is arrived at from the phase profile.

Figure 2 is a high resolution electron hologram of an undoped (electrically inactive) $\Sigma = 5$ (310) 36.8° symmetrical tilt GB in $SrTiO_3$, with a hologram fringe spacing of 0.09 nm, achieved by applying 180 V to the biprism. The zone axis on either side of the GB is [001], which ensures identical phase change in both the crystals provided the specimen thickness is the same across the GB (specimen thickness was measured using EELS, and the

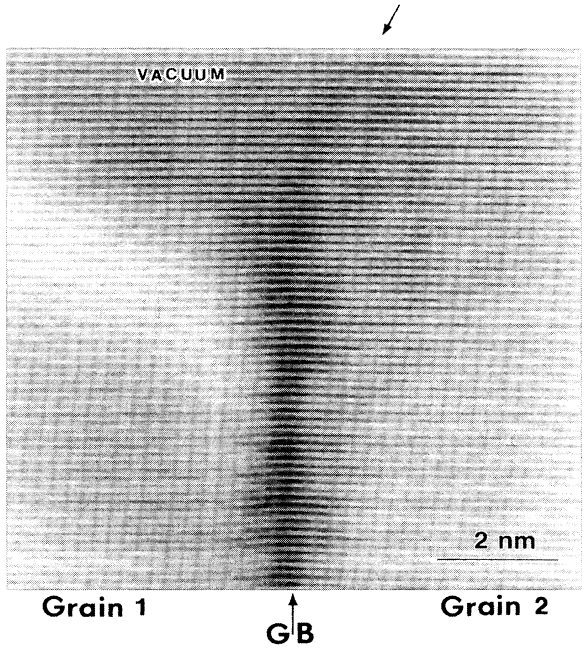

FIG. 5. An electron hologram of a Mn-doped GB in $SrTiO_3$. The fringe spacing is about 0.14 nm.

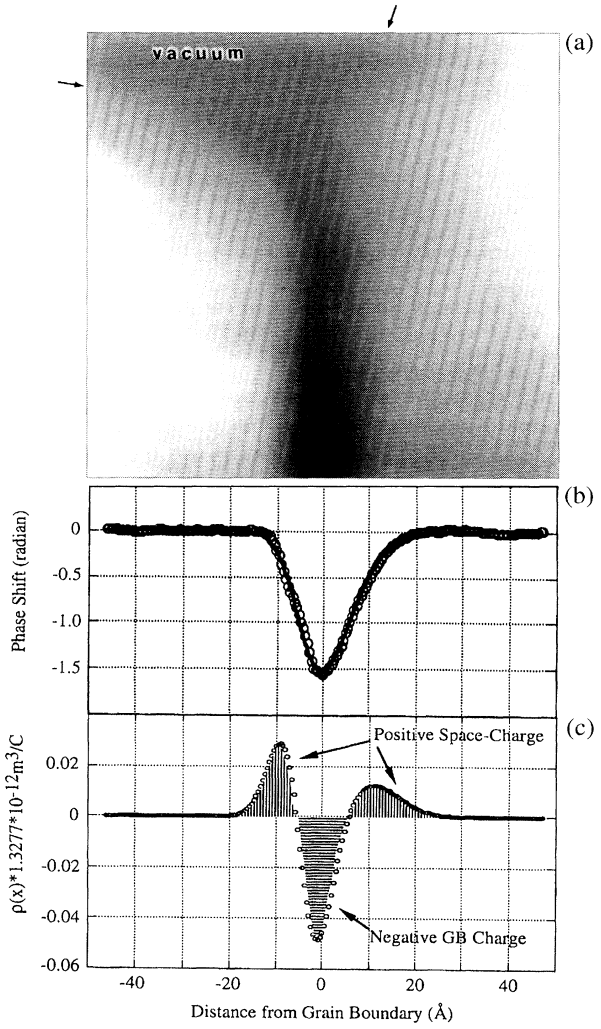

FIG. 6. (a) Phase reconstruction of the hologram in Fig. 5. (b) An averaged line profile across the GB shows a large decrease in phase at the GB, and the (c) resultant charge density profile indicates a negatively charged GB with positive space charge.

uniformity of thickness was confirmed to be within 10%). There is no extrinsic segregation or variation in cation stoichiometry across the GB [13]. The only phase change expected for such a GB is largely due to the reduction in mean inner potential (including any local strain effects) at the GB core. The reconstructed phase image (Fig. 3) is uniform, reaffirming that the thickness variation across the field of view is negligible with virtually no contrast at the GB. However, a line scan across the GB averaged along the symmetry axis of the interface (inset, Fig. 3) clearly indicates a small increase in phase at the GB core, i.e., the phase is "less delayed" at the GB core. This phase increase is likely because of a reduction in the mean inner potential due to the reduction in density of atoms at the GB core. The spatial extent of this phase change (1.8 ± 0.6 nm, from Fig. 3) and the observation of a reduction in the density of atoms at the GB are consistent with our prior results from Z-contrast imaging, column-by-column EELS spectroscopy (which yielded a GB width of 1.6 ± 0.4 nm) [14] and atomistic simulations [15]. The phase increase at several such undoped boundaries is extremely consistent and small, between 0.1 and 0.125 rad. This forms the basis for subsequent experiments on doped GBs where the phase change is substantially higher.

Depending on the solute type (donor versus acceptor) and processing history, the GB may be positively or negatively charged with opposite space charge. This provides a classic platform for electron holography with two possible scenarios, one of which is depicted in Fig. 4. Assuming that the charge at the GB is confined to atomic dimensions (i.e., a singularity in potential), the phase profiles and the derived charge density plots for a negatively charged GB (with positive space charge) would be as indicated in Fig. 4. Such a GB would result in a shift of the biprism interference fringes towards the reference vacuum. The shift of the fringes is directly proportional to the change in phase, which in turn is directly proportional to the electrostatic potential [16] arising in this case from the strength of the trapped electrical charge.

Figure 5 is an electron hologram of a Mn-doped GB in polycrystalline $SrTiO_3$, taken with both crystals under very weak diffraction conditions, with a hologram fringe spacing of 0.14 nm, achieved by applying 100 V to the biprism. Mn, added as a GB dopant in a second firing treatment, is found to be ubiquitous at all GBs and confined to the GB core [17]. The shifting of the electron biprism fringes at the GB core towards vacuum is evident, indicating a negative GB charge [see Fig. 4(a)]. The reconstructed phase image [Fig. 6(a)] is rich in information, and the corresponding line scan of phase across the GB, corrected for external phase shifts due to leakage fields [18], shows a substantial decrease in phase (–1.57 rad) at the GB core. This phase change is due to a combination of both an intrinsic change in the mean inner potential and a local electrostatic field. Under weak diffracting conditions, our measurements of many undoped GBs in polycrystals show that their phase change is on an average about 0.1 rad, which is too small to explain the large phase shift such as seen in Fig. 6. Though quite small, we extracted out the contribution associated with undoped GB from the corrected phase scan to extract the phase profile [Fig. 6(b)] solely due to the local electrostatic field. The phase profile thus obtained corresponds to a double Schottky barrier at the GB as projected on the specimen surface, assuming a uniform thickness of 48 nm (determined using EELS). Figure 6(c) is the charge density profile obtained from this phase profile using Poisson's equation, and it clearly shows the presence of negative charge centered at the GB core and a compensating positive space charge across the GB. This is the direct real space evidence for GB charge and compensating space charge.

TABLE I. Aspects of the double Schottky model derived from Mn-doped $SrTiO_3$ GB holograms.

Boundary number	Phase shift at GB ($\Delta\sigma$ rad)	Width of the space-charge region across GB (Å)	Schottky potential barrier height (V)
1	–1.56	46	–4.28
2	–1.67	43	–4.60
3	–0.36	72	–1.01
4	–0.29	55	–0.79
5	–0.23	60	–0.64

The presence of negative GB charge is consistent with our previous EELS studies, which indicated that Mn is present at the GB with a predominant valence of +2, with some +3 contribution [17]. With $Mn^{+2/+3}$ substitutionally replacing Ti at the GB core (due to size considerations), the defect reaction can be written as

$$Mn^{+2} + 2O_O{}^{x} \rightarrow Mn_{Ti}{}'' + 2V_O{}^{\bullet\bullet} + O_2,$$

$$Mn^{+3} + 2O_O{}^{x} \rightarrow Mn_{Ti}{}' + 2V_O{}^{\bullet\bullet} + O_2,$$

resulting in negatively charged defects Mn_{Ti}'' at the GB core, which are compensated by positively charged oxygen vacancies or holes. Thus, the inferred negative GB charge and corresponding positive space charge are consistent with direct measurements with electron holography.

All Mn-doped GBs studied consistently show negatively charged GBs with positive space charge. The spatial extent of the space-charge region was found to be about 3 nm on either side of the GB (see Table I), which is consistent with, albeit much smaller than, the typical Debye length reported in the literature [19]. This is probably due to the fact that Mn was diffused into the GB through a second firing treatment; thus the situation is one of nonequilibrium enrichment. However, a sizable variation in the magnitude of the phase decrease (and thus the double Schottky barrier height and the net charge) was observed for the various Mn-doped polycrystalline GBs, one extreme of which is Fig. 5. This variation clearly and directly shows that not all GBs in polycrystals are equally active, and the height of the double Schottky barrier is heterogeneous across the GBs. This observation is consistent with the results of Olsson and Dunlop [20] who found a large variation in the electrical transport properties across GBs in varistors, dictated by the potential at the GB. The space-charge profiles are often asymmetric about the GB core, which is expected due to the crystallographic anisotropy across polycrystalline GBs. The total charge, however, is completely compensated. The charge density profile yields the net charge accumulation at the GBs, which correspond to 35% to 45% substitution of Ti and Mn^{+2} at the core of the GB (i.e., the defect density of Mn_{Ti}'' is of the order of 10^{27} m^{-3} at the GB).

This Letter demonstrates that electron holography is a viable bulk sensitive tool to quantitatively probe the changes in electrostatic potential, and thus the magnitude, sign, and spatial extent of electrical charge at and across internal interfaces in solids. With the availability of *in situ I-V* specimen holders, it should be possible to perform similar measurements under dynamic conditions of current transport or applied electrical field.

Research supported by U.S. DOE (Contract No. DE-FG02-92ER45475). We thank Professor Waser and Dr. Vollmann for providing the Mn-doped samples.

[1] J. Frenkel, *Kinetic Theory of Liquids* (Oxford University Press, Oxford, 1946).
[2] J. Eshelby, C. Newey, P. Pratt, and A. Lidiard, Philos. Mag. **3**, 75 (1958).
[3] S. M. Sze, *Physics of Semiconductor Devices* (Wiley, New York, 1981).
[4] See *Grain Boundary Phenomena in Electroceramics, Advances in Ceramics Vol. 1,* edited by L. M. Levinson and D. C. Hill (American Ceramic Society, Columbus, OH, 1986).
[5] M. R. McCartney *et al.,* Appl. Phys. Lett. **65**, 2603 (1994).
[6] S. Frabboni, G. Matteucci, and G. Pozzi, Phys. Rev. Lett. **55**, 2196 (1985).
[7] Y-M. Chiang and T. Takagi, J. Am. Ceram. Soc. **73**, 3278 (1990); S. B. Desu and D. A. Payne, J. Am. Ceram. Soc. **73**, 3391 (1990); J. A. S. Ikeda and Y-M. Chiang, J. Am. Ceram. Soc. **76**, 2437 (1993).
[8] D. A. Bonnell and I. Solomon, Ultramicroscopy **42**, 788 (1992).
[9] G. Möllenstedt and H. Wahl, Naturwissenschaften **55**, 340 (1968).
[10] A. Tonomura, Rev. Mod. Phys. **59**, 639–668 (1987).
[11] M. Gajdardziska-Josifovska *et al.,* Ultramicroscopy **50**, 285 (1993).
[12] For example, M. Lehmann, E. Volkl, and F. Lenz, Ultramicroscopy **54**, 335 (1994).
[13] V. Ravikumar and V. P. Dravid, Ultramicroscopy **52**, 557 (1993).
[14] M. M. McGibbon *et al.,* Science **266**, 102 (1994).
[15] V. Ravikumar, D. Wolf, and V. P. Dravid (to be published).
[16] L. D. Landau and E. M. Lifsitz, *Quantum Mechanics* (Pergamon Press, London, 1965), pp. 153–155.
[17] N. Wilcox, V. Ravikumar, R. P. Rodrigues, and V. P. Dravid, Solid State Ionics **75**, 127 (1995).
[18] G. Pozzi, J. Phys. D (to be published).
[19] M. F. Yan, R. M. Cannon, and H. K. Bowen, J. Appl. Phys. **52**, 764 (1983).
[20] E. Olsson and G. L. Dunlop, J. Appl. Phys. **66**, 4317 (1989); E. Olsson and G. L. Dunlop, J. Appl. Phys. **66**, 3666 (1989).

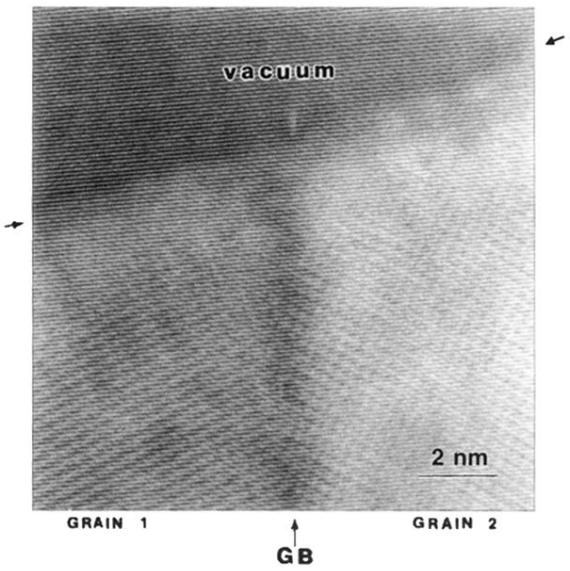

FIG. 2. An electron hologram of an undoped $\Sigma = 5$ (310) symmetrical tilt GB in $SrTiO_3$. Hologram interference fringe spacing $\approx$0.09 nm.

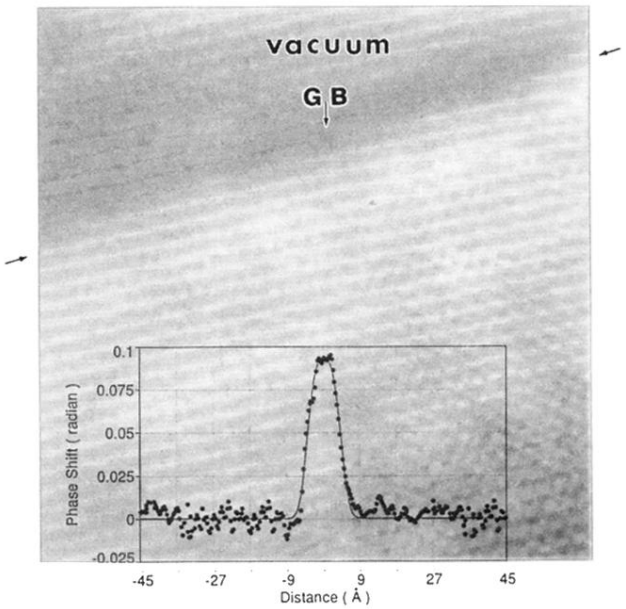

FIG. 3. Phase reconstruction of the hologram in Fig. 2. The averaged line scan of the phase across the GB is shown as an inset.

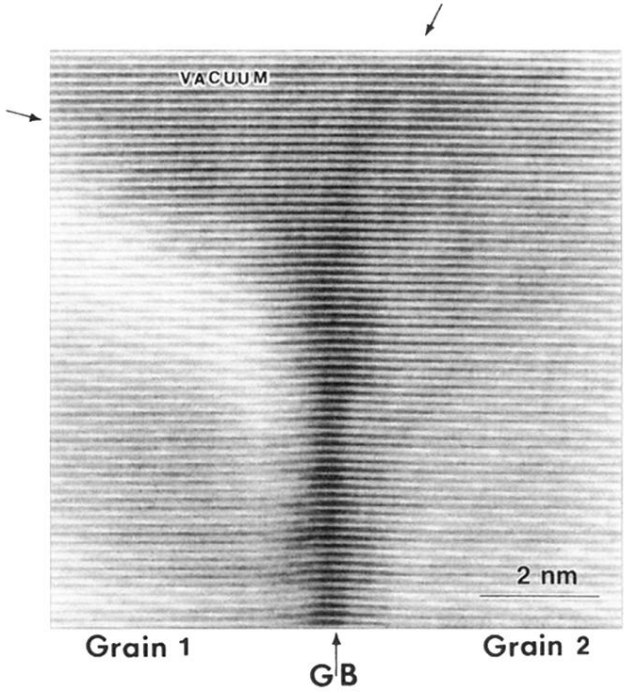

FIG. 5. An electron hologram of a Mn-doped GB in $SrTiO_3$. The fringe spacing is about 0.14 nm.

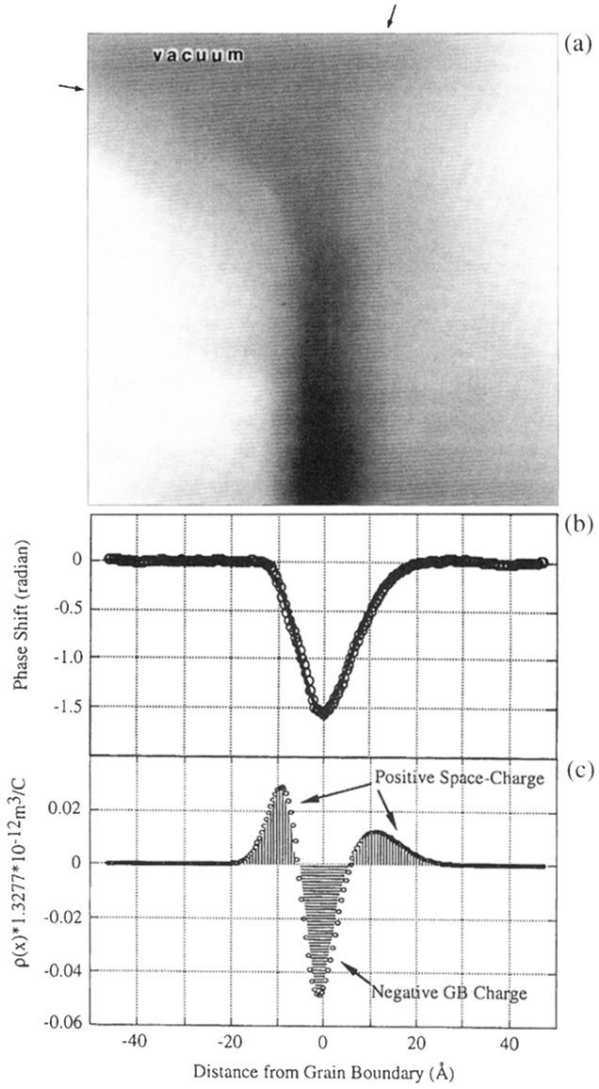

FIG. 6. (a) Phase reconstruction of the hologram in Fig. 5. (b) An averaged line profile across the GB shows a large decrease in phase at the GB, and the (c) resultant charge density profile indicates a negatively charged GB with positive space charge.